# Non-invasive Electrical Stimulation Upregulates Genes Encoding Melatonin-Related Machinery in Pineal and Salivary Glands, with Dermatome and Frequency-Specific Effects

**S. C. Lumsden**
University of Otago
**A. Clarkson**
University of Otago
**Yusuf Ozgur Cakmak** ( yusuf.cakmak@otago.ac.nz )
University of Otago

**Article**

**Keywords:** PG, melatonin, hydroxyindole-o-methyltransferase, gene expression, electric stimulation

**Posted Date:** April 13th, 2022

**DOI:** https://doi.org/10.21203/rs.3.rs-1511390/v1

# Abstract

Pineal Gland (PG) neuromodulation is possible via invasive, electrical stimulation of its sympathetic pathway. The present study aimed to investigate the potential of non-invasive neuromodulation of the pineal and salivary glands via electrical stimulation. Bilateral electrical stimulation at 10 or 80 Hz or sham stimulation was applied to either the C2 or T1 dermatomes of rats during the dark period for 2-hours. PG, salivary, and lacrimal glands were removed following stimulation and qPCR used to assess expression changes in genes associated with melatonin synthesis, regulation, and signalling. 80 Hz C2 dermatome stimulation significantly upregulated *Hiomt* within both the PG and submandibular glands, and *Rarβ* within PG only. 10 Hz C2 dermatome stimulation upregulated *Mt3* within the submandibular gland, and both 10 and 80 Hz C2 dermatome stimulation upregulated *Rorβ* within the parotid gland. Expression was unchanged following 10 or 80 Hz T1 dermatome stimulation and no changes were found in the lacrimal gland following stimulation of either dermatome. Our findings demonstrated that non-invasive, electrical stimulation can modulate gene expression within both the PG and salivary glands with frequency- and dermatome-specific effects. The potential therapeutic effects of this neuromodulation modality need to be uncovered through further research.


# 1.0 Introduction

The pineal gland (PG) is responsible for signalling darkness onset to the rest of the body via synthesis and secretion of the hormone, melatonin. Whilst several other extrapineal sites of melatonin synthesis exist [1], the PG is responsible for its nocturnal peak. Melatonin is synthesized in response to an absence of light detected by the retina. This information is transmitted via a multi-synaptic sympathetic pathway involving both the intermediolateral column of the spinal cord (IML)[2] and the superior cervical ganglia (SCG) (Fig. 1). The two key enzymes involved in the synthesis of melatonin are aralkylamine N-acetyltransferase (AANAT) and hydroxyindole-o-methyltransferase (HIOMT; Fig. 2).

Melatonin is a potent antioxidant and free-radical scavenger [3]. Reduction of peak night-time melatonin levels is associated with sleep disorders [4, 5] and neurodegenerative diseases [6–8]. The ‘melatonin replacement hypothesis’ postulates that restoration of the ‘normal’ melatonin night-time peak may help treat such diseases [9]. Oral melatonin supplements are one treatment option, however, the efficacy of these supplements is questionable due to inter-individual differences in melatonin profiles [10–12], meaning a one-fits-all dose cannot be applied. Moreover, melatonin’s half-life is very short, which raises questions around dose levels and how much is reaching target tissues. Further, melatonin supplements are not regulated by the Food and Drug Administration, and the actual dosage can vary greatly to that advertised on the packaging. Also, symptom aggravation can occur with these supplements in individuals with blood-clotting disorders, epilepsy [13], depression [14], and diabetes [15]. These issues advocate for alternative treatment options to restore endogenous melatonin levels.

Previous studies show modulation of AANAT, HIOMT, and therefore melatonin levels is possible via invasive electrical stimulation of the adrenergic pineal sympathetic innervation pathway [16]. However, using invasive stimulation with surgical intervention incurs substantial risk. If similar results are possible using non-invasive electrical stimulation, then this may have direct clinical applicability due to improved practicality and substantial risk reduction.

We identified the cervical and thoracic spinal nerve dermatomes as potential targets for non-invasive electrical stimulation of the pineal sympathetic pathway. Stimulation of these dermatomes may anterogradely stimulate corresponding spinal nerves and, in turn, sympathetic fibres associated with these spinal cord levels. This may stimulate structures directly implicated in the PG sympathetic pathway. The SCG contribute to the innervation of the C2-C4 dermatomes and inferior cervical ganglia (ICG) contribute to innervation of the C7, C8, T1, and T2 dermatomes [17, 18]. As the SCG are directly implicated in the PG sympathetic pathway, and pre-ganglionic fibres in this pathway ascend through the ICG to reach the SCG [18, 19], stimulation of dermatomes associated with these structures may stimulate the pineal sympathetic pathway. To test this, we investigate whether either 10 or 80 Hz non-invasive electrical stimulation of cervical and thoracic dermatomes are capable of modulating gene expression within the rat PG. We also investigate possible gene changes in the submandibular, parotid, and lacrimal glands due to them being similarly sympathetically innervated by the SCG.

# 3.0 Results

### 3.1 Reference Gene Selection

Although *B-actin* and *Hrpt* demonstrated the highest primer efficiencies out of the four reference genes investigated, the resulting melting curves showed non-specific amplification. *Rpl-13* showed the lowest efficiency out of all four genes tested and was therefore, not selected as a reference gene. *Gapdh* showed high efficiency with uniform melting curves indicating amplification of only the specific target sequence. Therefore, *Gapdh* was chosen as the reference gene for downstream analysis.

## 3.2 Pineal gland

Data for GOI are presented as fold-change in expression relative to the appropriate sham group (Fig. 3). All examined GOI were expressed in the PG in all the stimulation and sham groups, as previously reported. No significant differences were observed between experimental groups for *Aanat, Clock, Bmal1, Mt3, Per2, Rorβ, Tph1*, or *Cry1*. No significant differences were found for any genes with T1 dermatome stimulation (Figure S1 and Table S1). A significant upregulation in *Hiomt* ($p = 0.0142$, $F(2,27) = 5.27$, $n = 10$ for all groups) and *Rarβ* ($p = 0.0324$, $F(2,25) = 3.95$, $n = 9$ for all groups) expression was observed following 80 Hz stimulation of C2 dermatome compared to sham controls. This increased expression was approximately 1.5-fold for *Hiomt* and 2.5-fold for *Rarβ.*

## 3.3 Parotid Gland

In the sham groups, the Cq values for *Aanat, Hiomt, Bmal1, Mt3, Rarβ, Per2, Rorβ, Reve-erbα, Tph1*, and *Cry1* were all ≧ 33 (Table 1) and significantly higher than those of *Gapdh* ($p < 0.0001$, $n = 19$) indicating that usual expression of these genes within the parotid gland is very low in rats during the dark period.

Data for GOI expression following C2 dermatome stimulation are presented as fold-change in expression relative to the appropriate sham group (Fig. 4). There was an approximate three-fold increase in *Hiomt* expression following 10 Hz stimulation ($n = 10$) compared to sham ($n = 8$) ($p = 0.0487$, $F(2,23) = 0.0461$). There was also a significant increase in *Rorβ* expression following 10 Hz ($p = 0.0032$, $F(2,24) = 9.12$, $n = 10$) and 80 Hz ($p = 0.0023$, $F(2,24) = 9.12$, $n = 9$) stimulation compared to sham controls ($n = 8$). These increases were ~ 3-fold and ~ 2.5-fold, respectively. No differences were found for any other GOI for either 10 or 80 Hz stimulation. Similarly, no differences in gene expression were found following T1 dermatome stimulation in the parotid gland (Figure S2 and Table S2).

## 3.4 Submandibular Gland

Cq values for *Tph1* in the sham groups all exceeded 33 cycle thresholds indicating that its expression within the submandibular glands of rats is very low (Table 1).

As was found in the PG, an approximate 3.5-fold increase in expression for *Hiomt* was observed following 80 Hz ($n = 10$) stimulation compared to the sham group ($n = 10$) at the C2 dermatome ($p = 0.0205$; $F(2,28) = 4.16$; Fig. 5). An approximate 1.5-fold increase in expression was also found for *Mt3* following 10 Hz ($n = 11$) stimulation compared to sham ($n = 10$) at the C2 dermatome ($p = 0.0094$, $H = 8.29$; Fig. 6). No other significant changes in gene expression were found for any other GOI in the submandibular gland. No gene expression differences were found following T1 dermatome stimulation (Figure S3 and Table S3).

Table 1
**Average Cq values for sham stimulated groups for lowly expressed genes.**

| | Gene | Average Cq Value | *n* |
|---|---|---|---|
| **Parotid gland** | *Aanat* | 33.4 | 18 |
| | *Hiomt* | 33.4 | 16 |
| | *Bmal1* | 34.4 | 19 |
| | *Mt3* | 34.2 | 19 |
| | *Rarβ* | 34.5 | 19 |
| | *Per2* | 34.1 | 19 |
| | *Rorβ* | 34.1 | 17 |
| | *Rev-erbα* | 34.3 | 19 |
| | *Tph1* | 34.8 | 16 |
| | *Cry1* | 32.1 | 13 |
| **Submandibular gland** | *Tph1* | 33.9 | 19 |
| **Lacrimal gland** | *Aanat* | 30.5 | 17 |
| | *Hiomt* | 32.1 | 17 |

# 3.5 Lacrimal Gland

The average Cq value for the sham groups exceeded 30 cycle thresholds for *Aanat* and 32 cycle thresholds for *Hiomt* indicating that their expression within the rat lacrimal gland is very low. No differences in expression were found between any group or for any gene in the lacrimal gland (Figures S4,S5 and Tables S4, S5).

# 4.0 Discussion

Neuromodulation of key proteins within the PG is possible via invasive electrical stimulation of the sympathetic pathway [16]. Modulation of salivary proteins has also been shown through both invasive and non-invasive electrical stimulation [20–22]. However, ours is the most comprehensive study to date investigating both intracranial (PG) and extracranial (salivary and lacrimal glands) changes in gene expression in response to non-invasive electrical stimulation at different dermatomes and frequencies.

Our research shows stimulation at the C2 dermatome can modulate expression of genes encoding melatonin machinery with frequency-specific effects. These effects might be mediated via a transcriptional regulatory mechanism that encodes extracellular signals as bursts of nuclear localization of a transcription factor responsible for activating specific GOI [23]. In this manner, higher frequency stimulation is potentially necessary to stimulate both the pineal and submandibular glands' innervation pathways, and lower frequency stimulation favors that of the parotid gland. Indeed, low frequency (20 Hz) electrical stimulation can enhance parotid protein output in sheep [24] and high frequency (50 Hz) stimulation can increase saliva secretion from the submandibular gland in rats [25]. This frequency preference between the glands could be attributed to differing gene expression profiles that have been noted between the parotid and the submandibular glands [26, 27], which is supported by our data showing very low expression of GOI in the parotid gland and moderate expression in the submandibular gland. Such frequency-specific effects between structures are not unusual and have been documented extensively in previous literature surrounding neuromodulation.

We observed a change in *Hiomt* expression levels but saw no change in *Aanat*. Whilst *Aanat* upregulation is driven by adrenergic input from the post-ganglionic sympathetic fibres, HIOMT activity can be significantly increased *in vitro* via acute administration of neuropeptide Y (NPY)[28]. Moreover, no change in HIOMT activity occurs following administration of the β-adrenergic receptor agonist, isoproterenol, nor the $\alpha_1$-adrenergic receptor agonist, phenylephrine [28]. This suggests that, unlike AANAT, rapid changes in pineal HIOMT activity are regulated via a noradrenergic-independent mechanism. The PG possesses NPY-ergic fibres in a variety of

mammals such as the rat [29–31], Syrian hamster [32], guinea pig [33], cow [34], cat [35], monkey [36], and human [37]. Moreover, NPY is co-localized with NE in perivascular, sympathetic nerve terminals [38, 39]. The SCG provides perivascular innervation to the pineal as perivascular nerve terminals disappear from the gland following bilateral SCG-ectomy [40, 41]. Release of NPY from such terminals shows a preference for receiving stimulation at a higher frequency compared to lower frequency [42]. NPY is known to inhibit pineal melatonin release via inhibiting the stimulatory effect of NE on pinealocytes [43–45]. In this context, 80 Hz stimulation at the C2 dermatome in rats is potentially exerting its effect through the sympathetic innervation route of the PG via a potential NPY-ergic mechanism, causing an increase in *Hiomt* expression.

A previous study by Brownstein and Heller found a decrease in HIOMT levels following invasive stimulation of the preganglionic sympathetic fibres [46]. Methodological differences likely account for why we instead found an increase in *Hiomt* expression. Firstly, they stimulated at a frequency of 10 Hz, whereas we observed no change following 10 Hz and a significant upregulation with 80 Hz. This indicates higher frequencies can induce an stimulatory effect on *Hiomt*, whereas lower frequencies cannot, further emphasizing frequency-specific effects on pineal neuromodulation. Secondly, Brownstein and Heller found a decline in HIOMT levels with stimulation periods greater than two hours and did not sacrifice animals immediately following stimulation cessation, whereas we stimulated for two hours and opted for immediate sacrifice. Waiting one hour prior to sacrificing stimulated animals causes AANAT levels to decline [47] indicating that without immediate sacrifice and extraction of pineals following stimulation, any increase in AANAT levels might not be observable. Moreover, two hours of stimulation optimally upregulates AANAT levels, with a decline observed following three hours of stimulation [47]. Based on these observations, longer stimulation times offer a further explanation for why Brownstein and Heller observed a decrease in HIOMT levels.

Modulatory effects of C2 dermatome stimulation on the salivary glands are likely due to them receiving sympathetic innervation from the SCG which are also associated with innervation of the C2 dermatome, as previously described. The lack of any modulatory effects via T1 dermatome stimulation may be due to the absence of such anatomical connections between the T1 level of the spinal cord and these glands. Previous invasive stimulation studies all utilized either pre- or post-ganglionic fibres or the cervical sympathetic trunks [16] and, to the best of our knowledge, no other studies have attempted to non-invasively stimulate the SCG and ICG separately via their corresponding dermatomes.

Retinoic acid is a potent transcriptional and translational regulator [48], involved in signalling and regulation within the PG [49]. *Rarβ* is a noted tumor suppressor gene [50] and encodes for a retinoic acid receptor. Its expression is either low or silenced in various cancerous cells [51–57] and its increase in expression in these cells increases their sensitivity to chemotherapeutic agents, making it an ideal chemosensitisation target [58]. As 80 Hz stimulation at the C2 dermatome was able to significantly upregulate *Rarβ* expression within the PG, utilization of this effect to may help sensitize PG tumours to chemotherapeutic agents and improve the likelihood of positive treatment outcomes.

With regards to our upregulation of *Rorβ* in the parotid gland, this effect was observed following both 10 and 80 Hz stimulation indicating that this effect is not frequency-specific, but dermatome-specific. Retinoic acid-related orphan receptors (RORs) are a subfamily of nuclear hormone receptors for which a high-affinity, endogenous ligand has not been identified. RORs are not only involved in the modulation of circadian rhythms but also have important roles in the progression of certain cancers as both a tumour suppressor agent [59] and a tumour-promoting agent [60]. Research into *Rorβ* functioning and activity in this regard is still in its infancy with no clear identification of its role in oncogenesis and cancer progression. Therefore, the extent of the clinical significance for the increase in expression in the parotid gland in this study cannot yet be identified.

Our 10 Hz stimulation increased *Mt3* expression in the submandibular gland. Whilst named as a third melatonin receptor, MT3 has a greater affinity for the melatonin precursor NAS [61]. NAS has greater antioxidant and free-radical scavenging abilities than even melatonin [62–64] and this antioxidant effect might be mediated via the MT3 receptor [65–68]. There exists evidence for melatonin-independent roles for NAS *in vivo* as it can activate the tropomyosin receptor kinase B receptor which is involved in mediating the effects of brain-derived neurotrophic factor, whereas melatonin cannot [69]. Further, as much as 15% of melatonin synthesized is converted back to NAS [70, 71] and both NAS and melatonin are secreted from the PG [72]. Since it has previously been shown that melatonin is synthesized and likely secreted from the submandibular glands [73, 74], they may also secrete NAS. If this is true, then perhaps our 10 Hz stimulation at the C2 dermatome may promote an antioxidant effect via increased NAS signalling. Further, as brain-derived neurotrophic factor decreases with age [75, 76] and is also a potent regulator of plasticity [77, 78], it plausible to suggest that low frequency stimulation of the C2 dermatome could have potential as an adjunct for dementia prevention [79].

The overall low expression of most of our GOI within the parotid gland suggests that the synthesis, regulation, and signalling of melatonin within this gland is extremely low during the night. Moreover, despite melatonin being present in human tears [80] and the presence of AANAT, HIOMT with the lacrimal glands of Syrian hamsters [81], our experiments indicate that the expression of both *Aanat* and *Hiomt* within the lacrimal gland are also extremely low. This suggests that the rat lacrimal gland is not an extrapineal site of melatonin synthesis during the night, thus explaining a lack of any modulatory effect observed here.

Due to the tiny size of the PG, utilization of the whole gland for RNA extraction was necessary to collect enough total RNA for downstream analysis by qPCR. This meant there was not enough tissue available for assaying protein levels. As gene expression does not necessarily directly equate to protein levels, with correlation between the two estimated to be as little as 40% [82, 83], our study is limited to only making inferences regarding modulatory changes in gene expression. Therefore, for example, whilst we may have observed an increase in *Hiomt* expression, this might not necessarily equate to an increase in HIOMT activity.

Further, as our experiments were conducted in rats, any clinical implications drawn from our findings are merely speculative as there is no guarantee that similar results would be achieved with the same stimulation in humans. Therefore, future work is necessary to determine whether the results can be replicated in humans, and whether the stimulation protocols are able to elicit changes in both gene expression, corresponding protein levels, and what effect this may have on subsequent melatonin levels.

We have shown that non-invasive electrical stimulation of the C2 dermatome can modulate gene expression within the pineal, submandibular, and parotid glands with frequency-specific effects. Also, to the best of our knowledge, we have demonstrated the expression levels of *Mt3, Rorβ, Tph1* within the submandibular gland; *Hiomt*, *Clock, Bmal1, Mt3, Rarβ, Rorβ, Rev-erbα, Tph1, Cry1*, within the parotid gland, and *Aanat*, *Hiomt, Gapdh, Mt3, Rorβ, Rev-erba*, and *Tph1* within the lacrimal gland of the rat for the first time. As *Aanat* expression did not change with stimulation, our findings offer further evidence of a non-adrenergic innervation pathway to the PG through which *Hiomt* expression is regulated. This may occur through a NPY-ergic mechanism. These results have potential clinical applications in the sensitization of pineal tumour cells to chemotherapeutic agents via *Rarβ* upregulation. Future directions for this research should investigate the mechanism behind such upregulation, if changes in gene expression correspond to changes in protein levels within the same glands, and whether clinical translation of these findings is possible.

## 2.0 Methods

# 2.1 Animals

Male Wistar rats (2–3 months old; 300–550 g)(n = 54) were allowed access to food and water *ad libitum*. Animals were group housed in reverse 12-h light:12-h dark cycle (lights on 19:00–07:00). During the light phase, animals were exposed to cool, white, fluorescent light. During the dark phase, animals were exposed to complete darkness (light sources eliminated using blackout fabric). Animals were acclimatized to the light cycle for at least two weeks prior to experimental manipulation. All procedures for animal use were approved by the University of Otago animal ethics committee. All animals were procured from the Biomedical Resource Facility at the University of Otago and the study was carried out in compliance with the ARRIVE guidelines.

# 2.2 Transcutaneous Electrical Nerve Stimulation Experiments

Animals were randomly assigned to an experimental group: sham, 10 Hz, or 80 Hz stimulation at either the C2 or T1 dermatomes. We chose to investigate the C2 and T1 dermatomes, due to their interconnectivity with the SCG and ICG, respectively. Dermatome stimulation sites were determined based on rat dermatome maps [84] and are detailed in Fig. 6. As neighbouring rat dermatomes have overlapping borders, the C3, the lower cervical/upper thoracic dermatomes contributed to our C2 and T1 stimulation sites, respectively. However, as they are sympathetically innervated by the SCG (C3) or related with the ICG (cervical/upper thoracic) any non-specificity does not impose any limitations on results.

Animals were exposed to bright light (170–220 Lux) for 30-minutes to lower melatonin levels. Animals were then anaesthetized (isoflurane) and subjected to either active stimulation using a frequency of either 10 or 80 Hz, or sham stimulation at either C2 or T1 dermatomes for a period of two hours. Active stimulation used a current of 2 mA via a transcutaneous electrical nerve stimulation device (Acus 4, Cefar; Lund, Sweden). Sham stimulation involved placement of electrodes without any current being passed. Animals were then sacrificed via overdose of inhalation anaesthetic, and pineal, submandibular, parotid, and lacrimal glands immediately collected and frozen on dry ice.

2.3.Real-Time Quantitative PCR (qPCR)

## 2.3.1 RNA Precipitation and Extraction

Entire pineal and left parotid, submandibular, and lacrimal glands were used for downstream analysis. Harvested glands were washed in PBS solution to remove any residual blood. RNA extraction was performed using commercially available RNeasy Plus Mini kits (Qiagen, Germany) as per manufacturer's instructions. Eluted RNA was immediately placed on ice for quantification.

## 2.3.2 RNA Quantification

Total RNA was spectrophotometrically quantified using a Nanodrop 2000. Absorbance measurements were taken at 260 nm (minimum acceptable value = 1.75). Following quantification, all RNA was stored at -80°C until used for cDNA synthesis.

## 2.3.3 cDNA Synthesis

Commercially available kits (SensiFast cDNA synthesis kit; Bioline, Australia) were used to synthesize cDNA. Each reaction well contained reverse transcriptase buffer (4 µl), reverse transcriptase (1 µl), calculated volumes of RNA, and RNase-free water to synthesize cDNA from 100 ng total RNA for pineal samples, and 1000 ng for all other tissue. Cycling conditions for cDNA synthesis were as follows: 25°C for 10 minutes (primer annealing), 42°C for 15 minutes followed by 48°C for 15 minutes (reverse transcription), 85°C for 5 minutes (inactivation), and 4°C until sample removal (holding temperature). Synthesized cDNA was diluted with RNase-free water for (30 µL pineal samples and 10 µL for all other samples) to increase the total volume available for qPCR.

## 2.3.4 Primers

Genes of interest (GOI) were: *Aanat/Snat, Hiomt/Asmt, Clock, Bmal1/Arntl, Rarβ, Rorβ/Nr1f2/Rzrβ, Rev-erbα/Nrd1, Tph1, Mt3/QR2*, and *Cry1.* All GOI are expressed in the rodent PG [49, 85–90] apart from *Mt3*. GOI were chosen to examine any expression changes relating to melatonin synthesis, regulation, and signalling. Although expression has not been confirmed in the rodent PG, *Mt3* was also chosen as a GOI due to its high affinity for binding NAS [61], which is also secreted from the PG [91]. Primers were selected from existing literature and ran though Primer BLAST to check specificity. Forward and reverse primers are detailed in Table 2. *B-actin, Hprt, Rpl-13*, and *Gapdh* were investigated for suitability as reference genes. All primers were diluted with RNAse-free water (final concentration of 100 µM). Standard curves were generated for each GOI via 2:1 serial dilutions of cDNA derived from pineal tissue and from these, primer efficiencies were calculated.

Table 2
Forward and reverse primer sequences for all genes of interest.

| Gene | Forward Primer Sequence (5'-3') | Reverse Primer Sequence (5'-3') | Amplicon Length (bp) | Gene Accession Number/NCBI Number | Efficiency (%) |
|---|---|---|---|---|---|
| *Aanat* | GCGCGAAGCCTTTATCTCAGTCTCG | AGGCCACAAGACAGCCCTCCT | 122 | NM_012818.2 | 93.7 |
| *Hiomt* | GGTAGCTCCGTGTGT GTC TT | GAAGTCACCAGCGACAAACC | 108 | L78306 | 91.1 |
| *Clock* | CCACAACAGTTC TTA CAGACATCTC | AGGAGGGAAAGTGCTCTGTTG | 101 | NM_021856 | 97.4 |
| *Bmal1* | CGGGCGACTGCACTCACACA | GCCAAAATAGCCGTCGCCCTCT | 135 | NM_024362.2 | 95.3 |
| *Mt3* | TGG GAT AGA AGC CTA TGA AGC CTA C | GGATTGCTGGAACGCTGAAC | 134 | NM_001004214.1 | 95.8 |
| *Rarβ* | ACACCACGAATTCCAGCGCTGAC | CAGACCTGTGAAGCCCGGCA | 134 | NM_031529.1 | 100.6 |
| *Per2* | GCAGCCTTTCGATTATTCTCCC | GGACCAGCTAGTGTCCAGTGTG | 75 | NM_031678.1 | 87.7 |
| *Rorβ* | CCTTCCTCTCTGCAACTGAACA | AAGAAAGAAAGGCGGCATGG | 110 | NM_001270958.1 | 94.9 |
| *Rev-erbα* | AGGTGACCCTGCTTAAGGCTG | ACTGTCTGGTCCTTCACGTTGA | 81 | NM_145775.1 | 92.8 |
| *Tph1* | CTCTTGGAGCTTCAGAGGAGAC | GACTCTCAGCTGCCCATCTTG | 98 | NM_001100634 | 92.1 |
| *Cry1* | TTCGCCGGCTCTTCCAA | ATTGGCATCAAGGTCCTCAAGA | 74 | NM_198750.2 | 87.4 |
| *Gapdh* | GGGCTCTCTGCTCCTCCCTGT | CAGGCGTCCGATACGGCCAAA | 119 | NM_017008.4 | 96.2 |
| *B-actin* | CCCGCGAGTACAACCTTCTTG | GTCATCCATGGCGAACTGGTG | 71 | NM_031144.3 | 99.1 |
| *Hprt* | GTCATGTCGACCCTCAGTCC | GCAAGTCTTTCAGTCCTGTCC | 752 | NM_012583.2 | 100.3 |
| *Rpl-13* | AAGATCCGCAGACGCAAGG | TGCGTGCCATTTTCTTGTGG | 184 | NM_031101.1 | 80.7 |

## 2.3.5 Plate Setup and Cycling Parameters

qPCR was carried out in 96-well plates. Master mixes for each GOI were created for each plate. Each well contained a total reaction volume of 20 µl comprising: cDNA (3 µl), SensiFAST SYBR green Lo-ROX (10 µl), forward primer (0.2 µl), reverse primer (0.2 µl), and RNase-free water (6.6 µl). All samples were assayed in triplicate, or duplicate when this was not possible. Controls for each plate were wells containing RNase-free water only (20 µL), and 'no template control' wells containing all the reaction components listed above except for cDNA which was substituted for an equivalent volume of RNase-free water. The cycling protocol for the LightCycler 480 (Roche; Switzerland) is detailed in Table 3.

Table 3
**Cycling conditions for qPCR.**

| Programme Name | Cycles | Analysis Mode | Target (°C) | Analysis Mode | Hold (mm:ss) | Ramp Rate (°C/s) | Acquisition (per °C) | Sec Target (°C) | Step Size (°C) | Step Delay (cycles) |
|---|---|---|---|---|---|---|---|---|---|---|
| Pre-incubation | 1 | None | 95 | None | 02:00 | 4.4 | / | 0 | 0 | 0 |
| Amplification | 40 | Quantification | 95 | None | 00:05 | 4.4 | / | 0 | 0 | 0 |
| | | | 65 | None | 00:10 | 2.2 | / | 0 | 0 | 0 |
| | | | 72 | Single | 00:15 | 4.4 | / | 0 | 0 | 0 |
| Melt Curve Analysis | 1 | Melting Curves | 95 | None | 00:01 | 4.4 | / | 0 | 0 | 0 |
| | | | 50 | None | 01:00 | 2.2 | / | 0 | 0 | 0 |
| | | | 95 | Continuous | / | 0.10 | 6 | 0 | 0 | 0 |

## 2.4 Data Analysis

Raw Cq values were normalized to *Gapdh*, to calculate ΔCq values. ΔΔCq values and fold-changes in gene expression relative to sham stimulation were also calculated [92]. ΔCq values were used for hypothesis testing ($\alpha < 0.05$) which was carried out in GraphPad Prism 9. ΔΔCq values were used for graphical representation of fold-change differences between groups. Statistical significance was determined via one-way analysis of variance (ANOVA) with Tukey's multiple comparisons test for post-hoc testing for normally distributed data. For non-normally distributed data, the non-parametric Kruskal Wallis test was used followed by Dunn's multiple comparisons test for post-hoc testing.

## Declarations

**Data Availability:** The datasets generated during and/or analysed during the current study are available from the corresponding author on reasonable request.

**Sources of financial support:** This research was supported by the University of Otago PBRF research funds awarded to Drs Andrew N. Clarkson and Yusuf O. Cakmak and did not receive any specific grant from funding agencies in the public, commercial, or not-for-profit sectors.

**Author contributions:** SCL: experimental design, data acquisition, data analysis, data interpretation, manuscript writing and editing; YOC: funding, conceptualization, experimental design, data interpretation, manuscript editing; AC: funding, conceptualization, experimental design, data interpretation, manuscript editing.

**Competing interests:** YOC is a shareholder in Stoparkinson LLC, US. YOC has numerous granted & pending patents on non-invasive neuromodulation. The remaining authors have no competing interests to declare.

**Ethics declarations:** All methods involving animals were performed in accordance withthe code of ethical conduct for the use of animals in research as dictated by the Animal Welfare.

## References

1. Acuna-Castroviejo, D., et al., Extrapineal Melatonin: Sources, Regulation, and Potential Functions. Cell Mol Life Sci, 2014. **71**(16): p. 2997–3025.
2. Vrang, N., P.J. Larsen, M. Moller, and J.D. Mikkelsen, Topographical Organization of the Rat Suprachiasmatic-Paraventricular Projection. J Comp Neurol, 1995. **353**(4): p. 585–603.
3. Reiter, R.J., et al., Melatonin as an Antioxidant: Under Promises but over Delivers. J Pineal Res, 2016. **61**(3): p. 253–278.
4. Haimov, I., et al., Sleep Disorders and Melatonin Rhythms in Elderly People. Br Med J, 1994. **309**(6948): p. 167–167.
5. Zisapel, N., New Perspectives on the Role of Melatonin in Human Sleep, Circadian Rhythms and Their Regulation. Br J Pharmacol, 2018. **175**(16): p. 3190–3199.
6. Liu, R.-Y., J.-N. Zhou, J. van Heerikhuize, M.A. Hofman, and D.F. Swaab, Decreased Melatonin Levels in Postmortem Cerebrospinal Fluid in Relation to Aging, Alzheimer's Disease, and Apolipoprotein E-E4/4 Genotype. The Journal of clinical endocrinology & metabolism, 1999. **84**(1): p. 323–327.
7. Reiter, R.J., et al., Melatonin as a Free Radical Scavenger: Implications for Aging and Age-Related Diseasesa. Ann N Y Acad Sci, 1994. **719**(1): p. 1–12.
8. Hu, S., G. Shen, S. Yin, W. Xu, and B. Hu, Melatonin and Tryptophan Circadian Profiles in Patients with Advanced Non-Small Cell Lung Cancer. Adv ther, 2009. **26**(9): p. 886–92.
9. Hughes, R.J., R.L. Sack, and A.J. Lewy, The Role of Melatonin and Circadian Phase in Age-Related Sleep-Maintenance Insomnia: Assessment in a Clinical Trial of Melatonin Replacement. Sleep, 1998. **21**(1): p. 52–68.
10. Lerchl, A. and C.J. Partsch, Reliable Analysis of Individual Human Melatonin Profiles by Complex Cosinor Analysis. J Pineal Res, 1994. **16**(2): p. 85–90.
11. Arendt, J., Melatonin and Human Rhythms. Chronobiol Int, 2006. **23**(1–2): p. 21–37.

12. Nolte, I., et al., Pineal Volume and Circadian Melatonin Profile in Healthy Volunteers: An Interdisciplinary Approach. J Magn Reson Imaging, 2009. **30**(3): p. 499–505.
13. Sheldon, S.H., Pro-Convulsant Effects of Oral Melatonin in Neurologically Disabled Children. The Lancet, 1998. **351**(9111): p. 1254.
14. Werneke, U., T. Turner, and S. Priebe, Complementary Medicines in Psychiatry: Review of Effectiveness and Safety. The British Journal of Psychiatry, 2006. **188**(2): p. 109–121.
15. Rubio-Sastre, P., F.A. Scheer, P. Gómez-Abellán, J.A. Madrid, and M. Garaulet, Acute Melatonin Administration in Humans Impairs Glucose Tolerance in Both the Morning and Evening. Sleep, 2014. **37**(10): p. 1715–1719.
16. Lumsden, S.C., A.N. Clarkson, and Y.O. Cakmak, Neuromodulation of the Pineal Gland Via Electrical Stimulation of Its Sympathetic Innervation Pathway. Front Neurosci, 2020. **14**: p. 264.
17. Hoffman, H.H., An Analysis of the Sympathetic Trunk and Rami in the Cervical and Upper Thoracic Regions in Man. Ann Surg, 1957. **145**(1): p. 94–103.
18. Netter, F.H., *The Netter Collection of Medical Illustrations: Nervous System - Anatomy and Physiology*. 1999: Elsevier - Health Sciences Division.
19. Gabella, G., *The Sympathetic Ganglia*, in *Structure of the Autonomic Nervous System*. 1976, Springer Netherlands: Dordrecht. p. 3–47.
20. Schneyer, C.A. and H.D. Hall, Effects of Varying Frequency of Sympathetic Stimulation on Chloride and Amylase Levels of Saliva Elicited from Rat Parotid Gland with Electrical Stimulation of Both Autonomic Nerves. Proc Soc Exp Biol Med, 1991. **196**(3): p. 333–337.
21. Suntrup-Krueger, S., et al., Electrical Pharyngeal Stimulation Increases Substance P Level in Saliva. Neurogastroenterol Motil, 2016. **28**(6): p. 855–860.
22. Warren, C.M., et al., The Neuromodulatory and Hormonal Effects of Transcutaneous Vagus Nerve Stimulation as Evidenced by Salivary Alpha Amylase, Salivary Cortisol, Pupil Diameter, and the P3 Event-Related Potential. Brain Stimulation, 2019. **12**(3): p. 635–642.
23. Cai, L., C.K. Dalal, and M.B. Elowitz, Frequency-Modulated Nuclear Localization Bursts Coordinate Gene Regulation. Nature, 2008. **455**(7212): p. 485-U16.
24. Edwards, A.V. and D.A. Titchen, Autonomic Control of Protein Production by the Parotid Gland of the Sheep. Auton neurosci, 2003. **103**(1–2): p. 38–49.
25. Garrett, J.R., X.S. Zhang, G.B. Proctor, and L.C. Anderson, Sequential Secretion of Rat Submandibular Kallikrein and Peroxidase During Intermittent Sympathetic Stimulation. J Auton Nerv Syst, 1996. **61**(1): p. 26–30.
26. Bedi, G.S., The Effect of Adrenergic Agonists and Antagonists on the Expression of Proteins in Rat Submandibular and Parotid Glands. Crit Rev Oral Biol Med, 1993. **4**(3): p. 565–571.
27. Sun, Q.F., Q.H. Sun, J. Du, and S. Wang, Differential Gene Expression Profiles of Normal Human Parotid and Submandibular Glands. Oral Dis, 2008. **14**(6): p. 500–509.
28. Ribelayga, C., P. Pevet, and V. Simonneaux, Adrenergic and Peptidergic Regulations of Hydroxyindole-O-Methyltransferase Activity in Rat Pineal Gland. Brain res, 1997. **777**(1–2): p. 247–250.
29. Schon, F., et al., Neuropeptide Y Innervation of the Rodent Pineal Gland and Cerebral Blood Vessels. Neurosci Lett, 1985. **57**(1): p. 65–71.
30. Reuss, S. and R.Y. Moore, Neuropeptide Y-Containing Neurons in the Rat Superior Cervical Ganglion: Projections to the Pineal Gland. J Pineal Res, 1989. **6**(4): p. 307–16.
31. Zhang, E.T., J.D. Mikkelsen, and M. Møller, Tyrosine Hydroxylase- and Neuropeptide Y-Immunoreactive Nerve Fibers in the Pineal Complex of Untreated Rats and Rats Following Removal of the Superior Cervical Ganglia. Cell Tissue Res, 1991. **265**(1): p. 63–71.
32. Schröder, H., Neuropeptide Y (Npy)-Like Immunoreactivity in Peripheral and Central Nerve Fibres of the Golden Hamster (Mesocricetus Auratus) with Special Respect to Pineal Gland Innervation. Histochemistry, 1986. **85**(4): p. 321–325.
33. Schröder, H. and L. Vollrath, Neuropeptide Y (Npy)-Like Immunoreactivity in the Guinea Pig Pineal Organ. Neurosci Lett, 1986. **63**(3): p. 285–289.

34. Phansuwan-Pujito, P., S. Pramaulkijja, P. Govitrapong, and M. Møller, An Immunohistochemical Study of Neuropeptide Y in the Bovine Pineal Gland. J Pineal Res, 1993. **15**(1): p. 53–58.
35. Møller, M., P. Phansuwan-Pujito, S. Pramaulkijja, N. Kotchabhakdi, and P. Govitrapong, Innervation of the Cat Pineal Gland by Neuropeptide Y-Immunoreactive Nerve Fibers: An Experimental Immunohistochemical Study. Cell Tissue Res, 1994. **276**(3): p. 545–550.
36. Mikkelsen, J.D. and G. Mick, Neuropeptide Y-Lmmunoreactive Nerve Fibres in the Pineal Gland of the Macaque (Macaca Fascicularis). J Neuroendocrinol, 1992. **4**(6): p. 681–688.
37. Moller, M., P. Phansuwan-Pujito, and C. Badiu, Neuropeptide Y in the Adult and Fetal Human Pineal Gland. Biomed Res Int, 2014: p. 7.
38. Lundberg, J.M., A. Anggard, J. Pernow, and T. Hokfelt, Neuropeptide Y-Immunoreactive, Substance P-Immunoreactive and Vip-Immunoreactive Nerves in Cat Spleen in Relation to Autonomic Vascular and Volume Control Cell Tissue Res, 1985. **239**(1): p. 9–18.
39. Clarke, J., et al., Interaction of Neuropeptide Y and the Sympathetic Nervous System in Vascular Control in Man. Circulation, 1991. **83**(3): p. 774–777.
40. Kappers, J.A., *Structure and Function of the Epiphysis Cerebri*. ed. J. Ariëns Kappers, et al. Vol. 10. 1965, Amsterdam, New York: Elsevier Pub. Co.
41. Hogendorf, P., E. Adamczyk, and E. Okraszewska, Microvascularisation of the Pineal Gland in the Rat. Folia Morphol (Warsz), 2001. **60**(3): p. 191–4.
42. Lundberg, J.M., A. Rudehill, A. Sollevi, E. Theodorsson-Norheim, and B. Hamberger, Frequency- and Reserpine-Dependent Chemical Coding of Sympathetic Transmission: Differential Release of Noradrenaline and Neuropeptide Y from Pig Spleen. Neurosci Lett, 1986. **63**(1): p. 96–100.
43. Wahlestedt, C., N. Yanaihara, and R. Håkanson, Evidence for Different Pre-and Post-Junctional Receptors for Neuropeptide Y and Related Peptides. Regul Pept, 1986. **13**(3–4): p. 307–18.
44. Olcese, J., Neuropeptide Y: An Endogenous Inhibitor of Norepinephrine-Stimulated Melatonin Secretion in the Rat Pineal Gland. J Neurochem, 1991. **57**(3): p. 943–947.
45. Simonneaux, V., A. Ouichou, C. Craft, and P. Pévet, Presynaptic and Postsynaptic Effects of Neuropeptide Y in the Rat Pineal Gland. J Neurochem, 1994. **62**(6): p. 2464–2471.
46. Brownstein, M.J. and A. Heller, Hydroxyindole-O-Methyl-Transferase Activity: Effect of Sympathetic Nerve Stimulation. Science, 1968. **162**(3851): p. 367–8.
47. Volkman, P.H. and A. Heller, Pineal N-Acetyltransferase Activity: Effect of Sympathetic Stimulation. Science, 1971. **173**(3999): p. 839–40.
48. Ransom, J., P.J. Morgan, P.J. McCaffery, and P.N. Stoney, The Rhythm of Retinoids in the Brain. J Neurochem, 2014. **129**(3): p. 366–376.
49. Ashton, A., P.N. Stoney, J. Ransom, and P. McCaffery, Rhythmic Diurnal synthesis and Signaling of Retinoic Acid in the Rat Pineal Gland and Its Action to Rapidly Downregulate Erk Phosphorylation. Mol Neurobiol, 2018. **55**(11): p. 8219–8235.
50. Xu, X.-C., Tumor-Suppressive Activity of Retinoic Acid Receptor-Beta in Cancer. Cancer letters, 2007. **253**(1): p. 14–24.
51. Liu, Z., et al., 5-Aza-2'-Deoxycytidine Induces Retinoic Acid Receptor-Beta(2) Demethylation and Growth Inhibition in Esophageal Squamous Carcinoma Cells. Cancer Lett, 2005. **230**(2): p. 271–83.
52. Brtko, J., Role of Retinoids and Their Cognate Nuclear Receptors in Breast Cancer Chemoprevention. Cent Eur J Public Health, 2007. **15**(1): p. 3–6.
53. Tang, D., et al., Methylation of the Rarb Gene Increases Prostate Cancer Risk in Black Americans. J Urol, 2013. **190**(1): p. 317–324.
54. Hua, F., et al., A Meta-Analysis of the Relationship between Rarβ Gene Promoter Methylation and Non-Small Cell Lung Cancer. PloS one, 2014. **9**(5): p. e96163-e96163.
55. Moison, C., et al., Synergistic Chromatin Repression of the Tumor Suppressor Gene Rarb in Human Prostate Cancers. Epigenetics, 2014. **9**(4): p. 477–482.
56. Viktorovna Kudryavtseva, A., et al., Upregulation of Rarb, Rarg, and Rorc Genes in Clear Cell Renal Cell Carcinoma. Biomed Pharmacol J, 2016. **9**(3): p. 967–975.

57. Yari, K. and Z. Rahimi, Promoter Methylation Status of the Retinoic Acid Receptor-Beta 2 Gene in Breast Cancer Patients: A Case Control Study and Systematic Review. Breast Care, 2019. **14**(2): p. 117–123.
58. Ren, H.-Y., B. Chen, G.-L. Huang, Y. Liu, and D.-Y. Shen, Upregulation of Retinoic Acid Receptor-B Reverses Drug Resistance in Cholangiocarcinoma Cells by Enhancing Susceptibility to Apoptosis. Mol Med Rep, 2016. **14**(4): p. 3602–3608.
59. Wen, Z.Z., et al., Ror Beta Suppresses the Sternness of Gastric Cancer Cells by Downregulating the Activity of the Wnt Signaling Pathway. Oncol Rep, 2021. **46**(2).
60. Matijevic, T. and J. Pavelic, The Dual Role of Tlr3 in Metastatic Cell Line. Clin Exp Metastasis, 2011. **28**(7): p. 701–712.
61. Nosjean, O., et al., Identification of the Melatonin-Binding Site Mt3 as the Quinone Reductase 2. J Biol Chem, 2000. **275**(40): p. 31311–7.
62. Seegar, H., A.O. Mueck, and T.H. Lippert, Effect of Melatonin and Metabolites on Copper-Mediated Oxidation of Flow Density Lipoprotein. Br J Clin Pharmacol, 1997. **44**(3): p. 283–4.
63. Karbownik, M., E. Gitto, A. Lewiñski, and R.J. Reiter, Relative Efficacies of Indole Antioxidants in Reducing Autoxidation and Iron-Induced Lipid Peroxidation in Hamster Testes. J Cell Biochem, 2001. **81**(4): p. 693–9.
64. Guajardo, M.H., A.M. Terrasa, and A. Catalá, Protective Effect of Indoleamines on in Vitro Ascorbate-Fe2 + Dependent Lipid Peroxidation of Rod Outer Segment Membranes of Bovine Retina. J Pineal Res, 2003. **35**(4): p. 276–82.
65. Sestini, E.A., J.C. Carlson, and R. Allsopp, The Effects of Ambient Temperature on Life Span, Lipid Peroxidation, Superoxide Dismutase, and Phospholipase A2 Activity in Drosophila Melanogaster. Exp Gerontol, 1991. **26**(4): p. 385–95.
66. Li, B., H. Zhang, M. Akbar, and H.Y. Kim, Negative Regulation of Cytosolic Phospholipase a(2) by Melatonin in the Rat Pineal Gland. The Biochemical journal, 2000. **351 Pt 3**(Pt 3): p. 709–716.
67. Kohen, R. and A. Nyska, Oxidation of Biological Systems: Oxidative Stress Phenomena, Antioxidants, Redox Reactions, and Methods for Their Quantification. Toxicol Pathol, 2002. **30**(6): p. 620–50.
68. Oxenkrug, G., Antioxidant Effects of N-Acetylserotonin: Possible Mechanisms and Clinical Implications. Ann N Y Acad Sci, 2005. **1053**: p. 334–47.
69. Jang, S.W., et al., N-Acetylserotonin Activates Trkb Receptor in a Circadian Rhythm. Proc Natl Acad Sci U S A, 2010. **107**(8): p. 3876–3881.
70. Leone, R.M. and R.E. Silman, Melatonin Can Be Differentially Metabolized in the Rat to Produce N-Acetylserotonin in Addition to 6-Hydroxy-Melatonin. Endocrinology, 1984. **114**(5): p. 1825–32.
71. Young, I.M., R.M. Leone, P. Francis, P. Stovell, and R.E. Silman, Melatonin Is Metabolized to N-Acetyl Serotonin and 6-Hydroxymelatonin in Man. J Clin Endocrinol Metab, 1985. **60**(1): p. 114–9.
72. Lee, B.H., et al., Two Indoleamines Are Secreted from Rat Pineal Gland at Night and Act on Melatonin Receptors but Are Not Night Hormones. J Pineal Res, 2020. **68**(2): p. e12622.
73. Shimozuma, M., et al., Expression and Cellular Localizaion of Melatonin-Synthesizing Enzymes in Rat and Human Salivary Glands. Histochem Cell Biol, 2011. **135**(4): p. 389–96.
74. Isola, M., M.A. Lilliu, F. Loy, and R. Isola, Diabetic Status Influences the Storage of Melatonin in Human Salivary Glands. The Anatomical Record, 2018. **301**(4): p. 711–716.
75. Hayashi, M., F. Mistunaga, K. Ohira, and K. Shimizu, Changes in Bdnf-Immunoreactive Structures in the Hippocampal Formation of the Aged Macaque Monkey. Brain res, 2001. **918**(1–2): p. 191–6.
76. Oh, H., D.A. Lewis, and E. Sibille, The Role of Bdnf in Age-Dependent Changes of Excitatory and Inhibitory Synaptic Markers in the Human Prefrontal Cortex. Neuropsychopharmacol, 2016. **41**(13): p. 3080–3091.
77. Mowla, S.J., et al., Differential Sorting of Nerve Growth Factor and Brain-Derived Neurotrophic Factor in Hippocampal Neurons. *J Neurosci*, 1999. **19**(6): p. 2069.
78. Berretta, A., Y.C. Tzeng, and A.N. Clarkson, Post-Stroke Recovery: The Role of Activity-Dependent Release of Brain-Derived Neurotrophic Factor. Expert Rev Neurother, 2014. **14**(11): p. 1335–44.
79. Weinstein, G., et al., Serum Brain-Derived Neurotrophic Factor and the Risk for Dementia: The Framingham Heart Study. JAMA neurology, 2014. **71**(1): p. 55–61.
80. Carracedo, G., et al., Presence of Melatonin in Human Tears. J Optom, 2017. **10**(1): p. 3–4.

81. Mhatre, M.C., A.S. van Jaarsveld, and R.J. Reiter, Melatonin in the Lacrimal Gland: First Demonstration and Experimental Manipulation. Biochem Biophys Res Commun, 1988. **153**(3): p. 1186–1192.
82. de Sousa Abreu, R., L.O. Penalva, E.M. Marcotte, and C. Vogel, Global Signatures of Protein and Mrna Expression Levels. Molecular BioSystems, 2009. **5**(12): p. 1512–1526.
83. Vogel, C. and E.M. Marcotte, Insights into the Regulation of Protein Abundance from Proteomic and Transcriptomic Analyses. Nat Rev Genet, 2012. **13**(4): p. 227–232.
84. Takahashi, Y. and Y. Nakajima, Dermatomes in the Rat Limbs as Determined by Antidromic Stimulation of Sensory C-Fibers in Spinal Nerves. Pain, 1996. **67**(1): p. 197–202.
85. Beckerandre, M., et al., Pineal-Gland Hormone Melatonin Binds and Activates an Orphan of the Nuclear Receptor Superfamily. J Biol Chem, 1994. **269**(46): p. 28531–28534.
86. Schaeren-Wierners, N., E. André, J.P. Kapfhammer, and M. Becker-André, The Expression Pattern of the Orphan Nuclear Receptor Rorβ in the Developing and Adult Rat Nervous System Suggests a Role in the Processing of Sensory Information and in Circadian Rhythm. Eur J Neurosci, 1997. **9**(12): p. 2687–2701.
87. Namihira, M., et al., Daily Variation and Light Responsiveness of Mammalian Clock Gene, Clock and Bmal1, Transcripts in the Pineal Body and Different Areas of Brain in Rats. Neurosci Lett, 1999. **267**(1): p. 69–72.
88. Nakamura, T.J., K. Shinohara, T. Funabashi, D. Mitsushima, and F. Kimura, Circadian and Photic Regulation of Cryptochrome Mrnas in the Rat Pineal Gland. Neuroscience res, 2001. **41**(1): p. 25–32.
89. Sugden, D., Comparison of Circadian Expression of Tryptophan Hydroxylase Isoform Mrnas in the Rat Pineal Gland Using Real-Time Pcr. J Neurochem, 2003. **86**(5): p. 1308–1311.
90. Andrade-Silva, J., J. Cipolla-Neto, and R.A. Peliciari-Garcia, The in Vitro Maintenance of Clock Genes Expression within the Rat Pineal Gland under Standard and Norepinephrine-Synchronized Stimulation. Neuroscience res, 2014. **81–82**: p. 1–10.
91. Lee, B.H., et al., Two Indoleamines Are Secreted from Rat Pineal Gland at Night and Act on Melatonin Receptors but Are Not Night Hormones. J Pineal Res, 2020. **68**(2): p. 14.
92. Livak, K.J. and T.D. Schmittgen, Analysis of Relative Gene Expression Data Using Real-Time Quantitative Pcr and the 2 − Δδct Method. Methods, 2001. **25**(4): p. 402–408.

## Figures

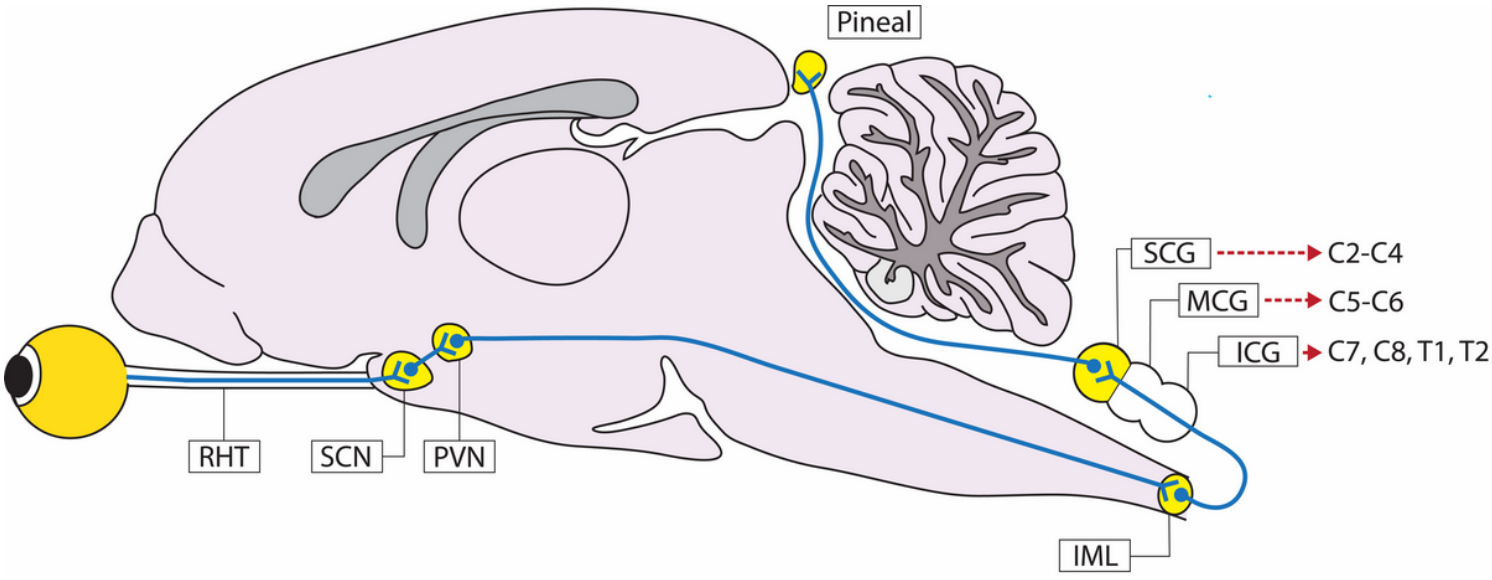


Figure 1

***Sympathetic pathway innervation of the PG.*** *An absence of light is detected by the eye which sends signals via the retinohypothalamic tract to the suprachiasmatic nucleus (SCN). From here, signals are sent to the paraventricular nucleus of the hypothalamus (PVN) and then the pathway descends the spinal cord to synapse at the intermediolateral column of the spinal cord (IML). Pre-ganglionic*

*sympathetic fibres that project from the IML ascend the spinal cord to synapse at the superior cervical ganglia (SCG) with post-ganglionic fibres that directly innervate the PG. This stimulates melatonin synthesis and secretion through release of norepinephrine. Yellow highlights structures involved in the pineal sympathetic innervation pathway, blue lines represent the flow of the pathway, and red dashed arrows represent flow to dermatome targets of the cervical ganglia.*

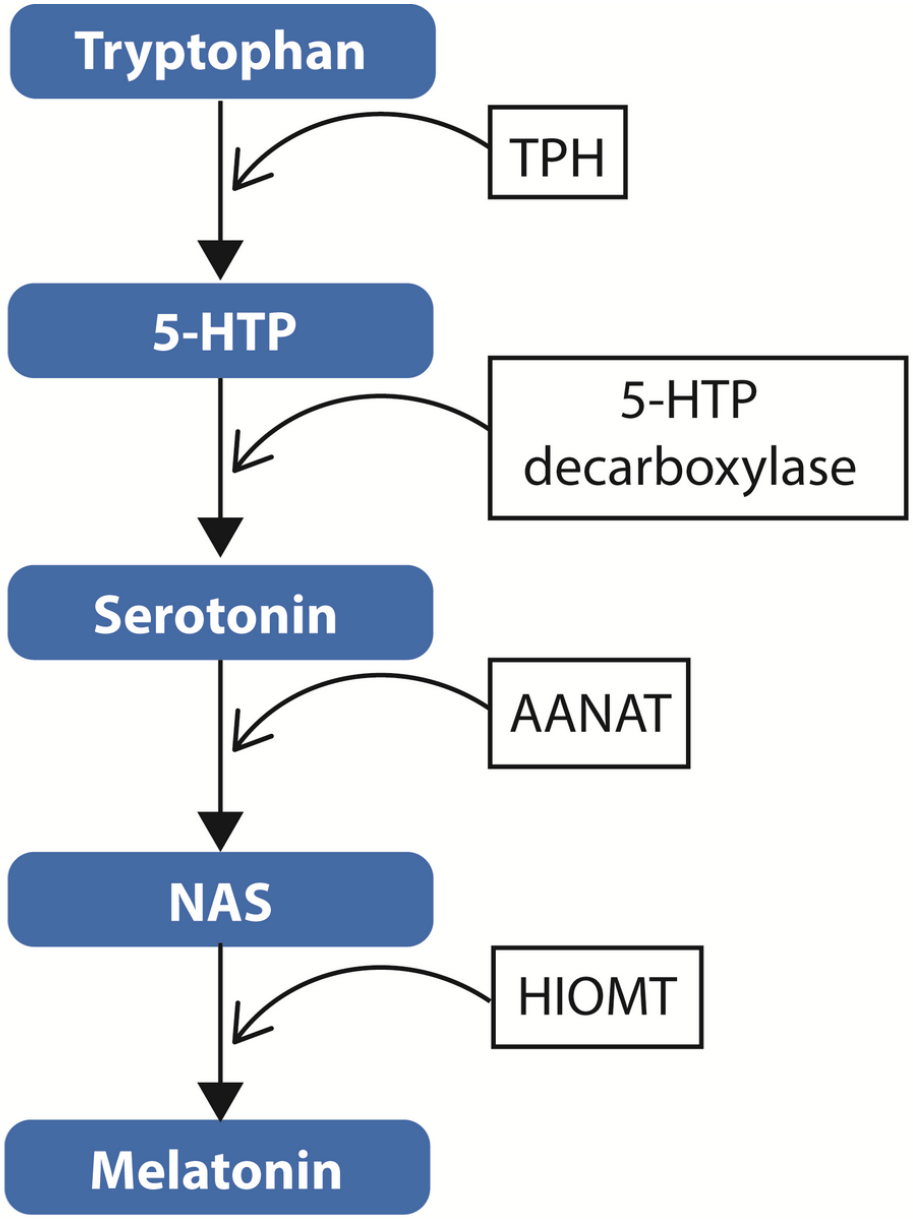


Figure 2

***Melatonin synthesis pathway.*** *Melatonin is synthesized via a multi-step pathway in which tryptophan is hydroxylated by trptophan-5-hydroxylase (TPH) to form 5-hydroxytryptophan (5-HTP). This is then decarboxylated by 5-HTP decarboxylase to form serotonin. Serotonin undergoes acetylation via the enzyme aralkylamine N-acetyltransferase (AANAT) to form N-acetylserotonin (NAS). NAS is acetylated by the enzyme hydroxyindole-o-methyltransferase (HIOMT) to form melatonin. The penultimate step involving AANAT in this pathway is generally considered to be the rate-limiting step.*

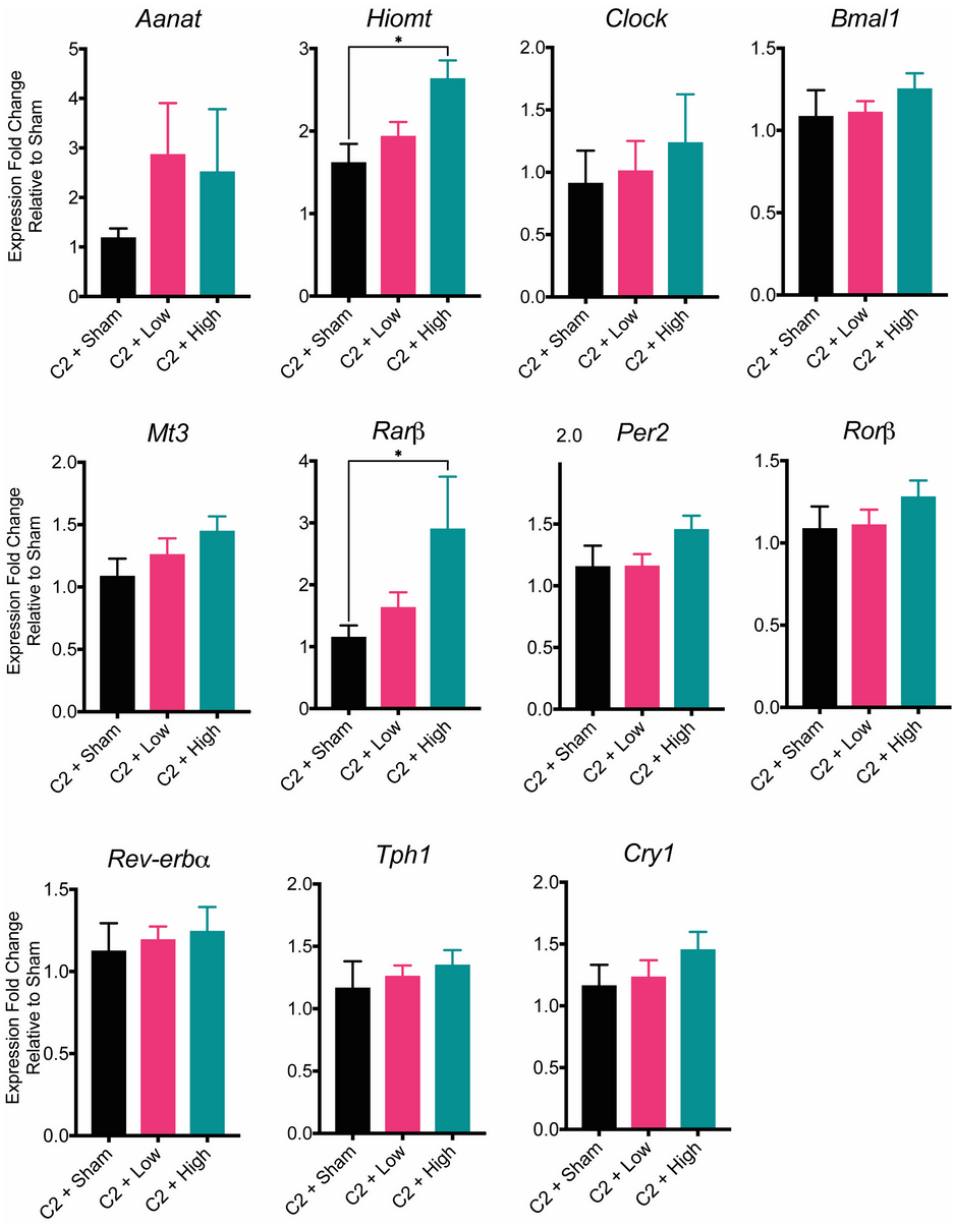


Figure 3

***Results from qPCR of PG samples of C2 dermatome stimulated rats.*** *Results are expressed as fold-change in expression relative to sham stimulated control ± SEM. Hypothesis testing and subsequent statistical significance refers to ΔCq values of GOI expression relative to reference gene expression (Gapdh). Expression of Hiomt and Rarβ is significantly upregulated in response to 80 Hz stimulation. 'Low': 10 Hz stimulation; 'High': 80 Hz stimulation; *= p <0.05.*

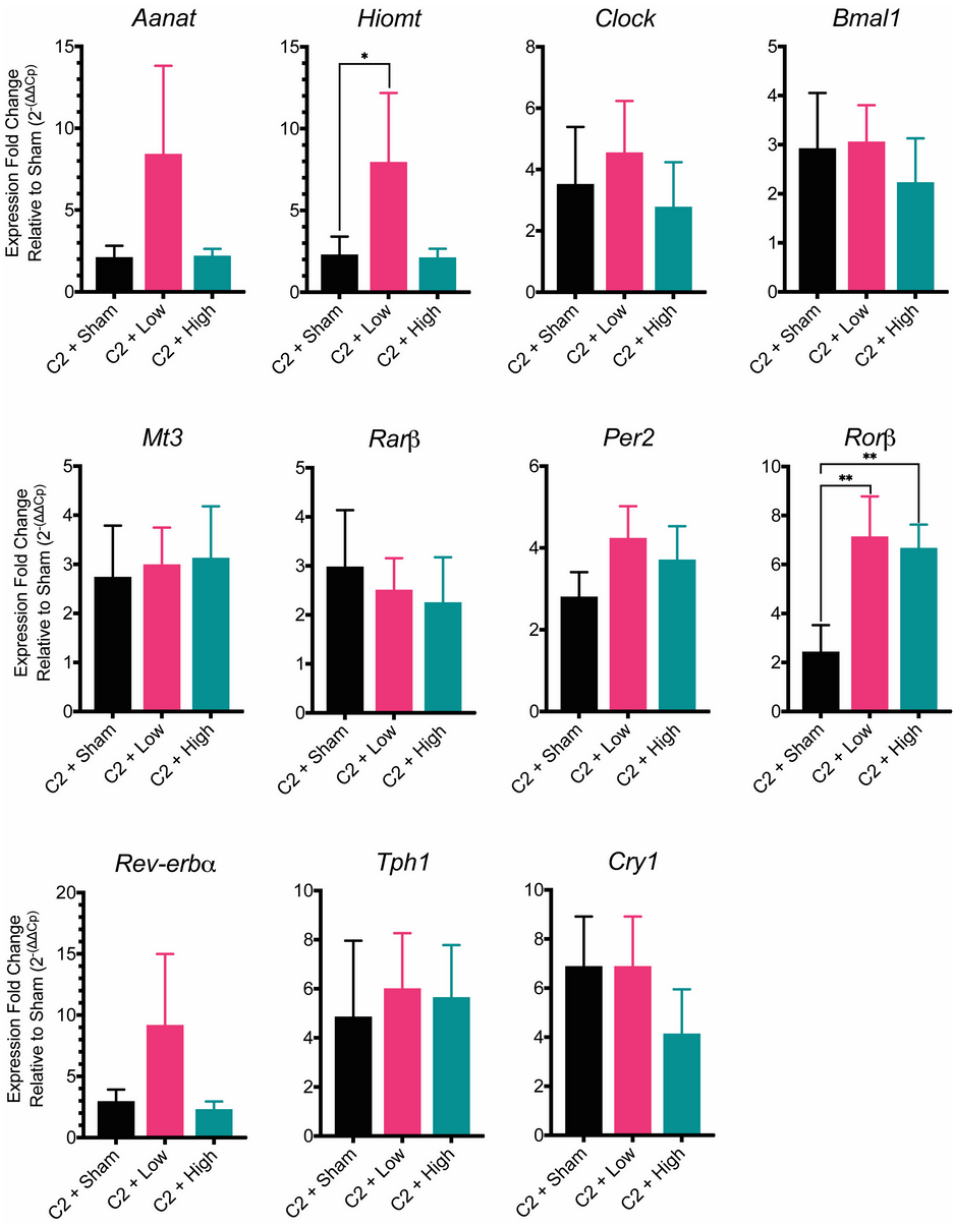


Figure 4

***Results from qPCR of parotid gland samples of C2 dermatome stimulated rats.*** *Results are expressed as fold-change in expression relative to sham stimulated control ± SEM. Hypothesis testing and subsequent statistical significance refers to ΔCq values of GOI expression relative to reference gene expression (Gapdh). Expression of Rorβ is significantly upregulated in response to both 10 Hz and 80 Hz stimulation. 'Low': 10 Hz stimulation; 'High': 80 Hz stimulation; * = p<0.05; ** = p<0.001.*

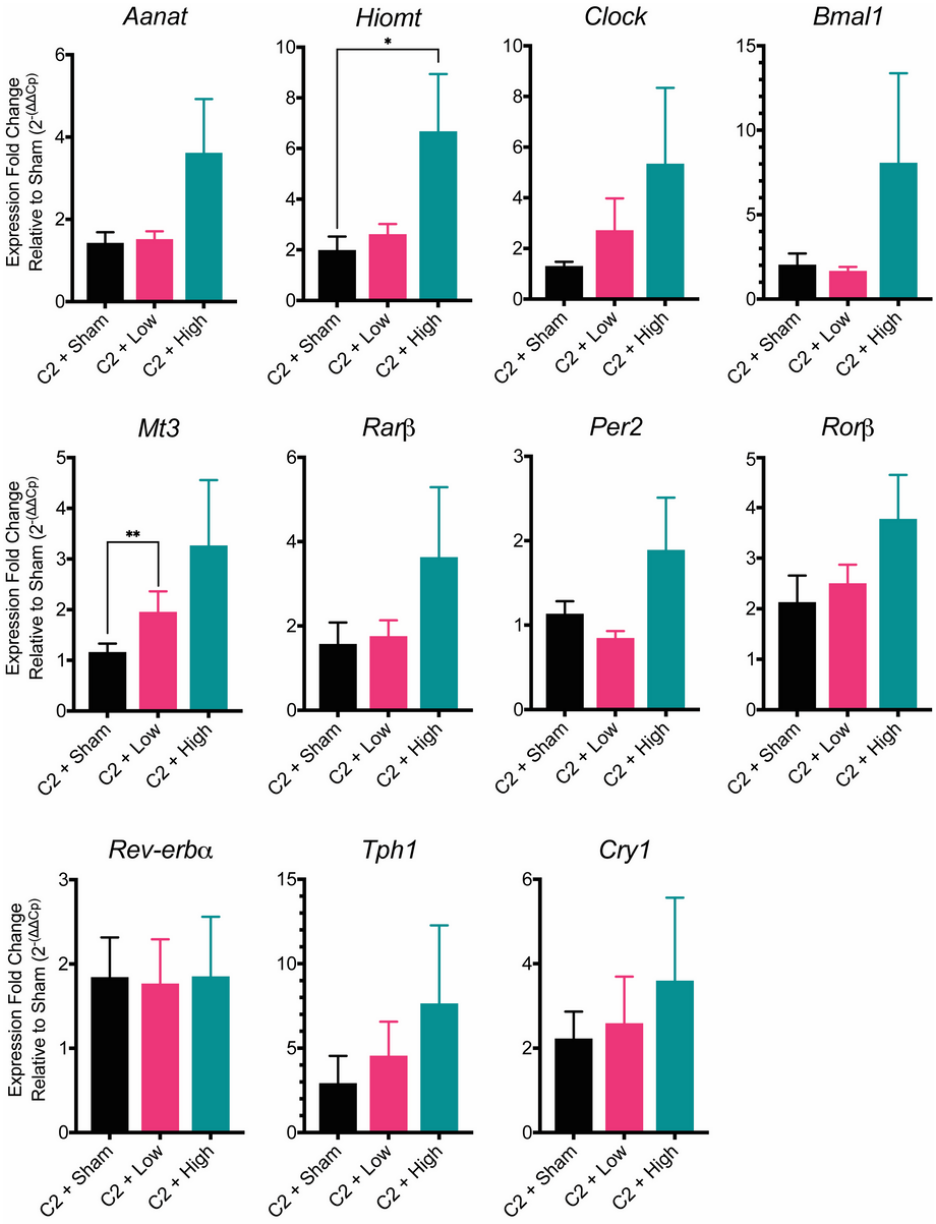


Figure 5

***Results from qPCR of submandibular gland samples of C2 dermatome stimulated rats.*** *Results are expressed as fold-change in expression relative to sham stimulated control ± SEM. Hypothesis testing and subsequent statistical significance refers to ΔCq values of GOI expression relative to reference gene expression (Gapdh). Expression of Hiomt is upregulated in response to 80 Hz stimulation whilst expression of Mt3 is upregulated following 10 Hz stimulation. 'Low': 10 Hz stimulation; 'High': 80 Hz stimulation; * = p<0.05.*

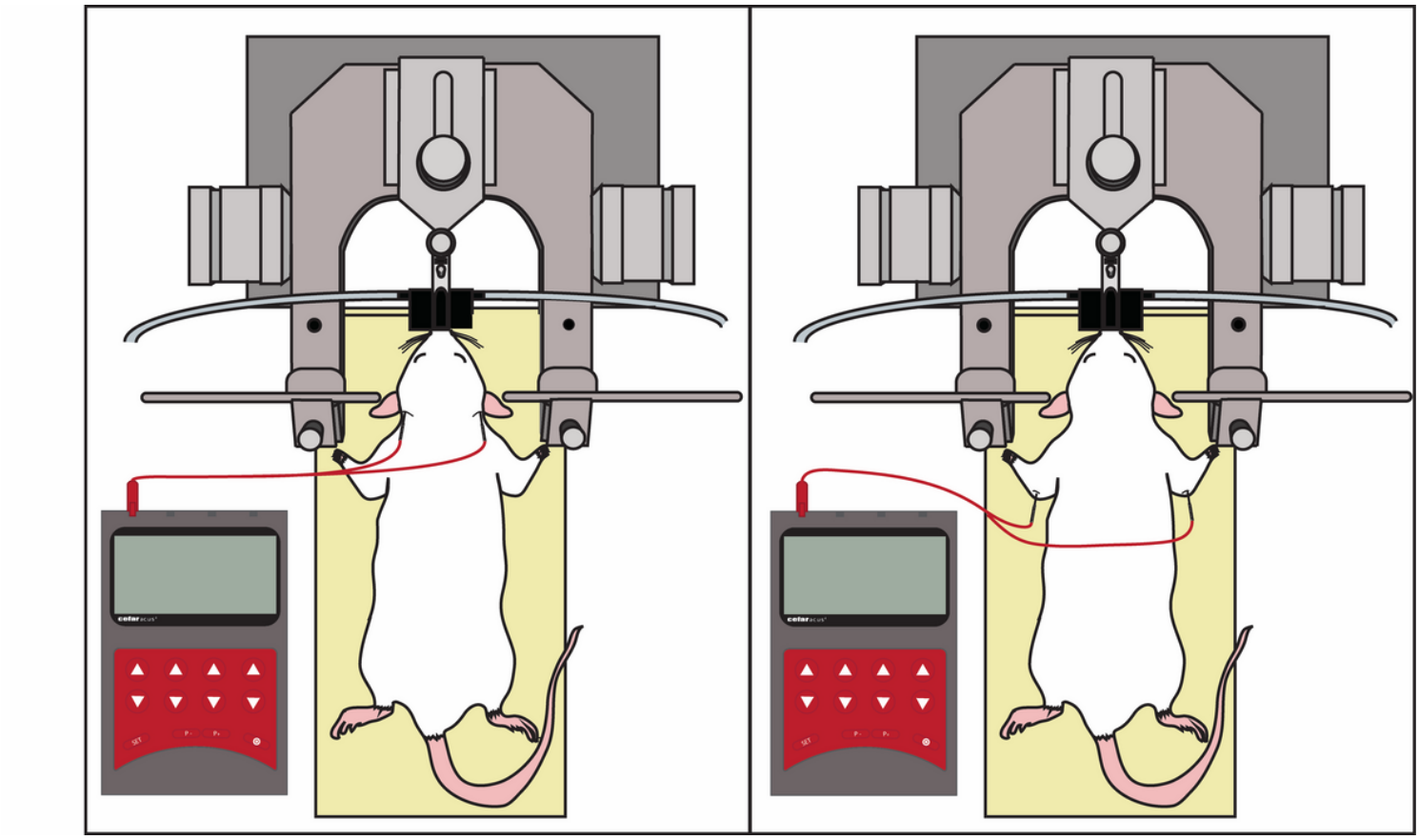

**Figure 6**

*Bilateral electrode placements for C2 (left panel) and T1 (right panel) dermatome stimulation.*

## Supplementary Files

This is a list of supplementary files associated with this preprint. Click to download.

- V1SupplementaryInformation.pdf